A ROBUST AND FAST IMAGING ALGORITHM WITHOUT DERIVATIVE OPERATIONS FOR UWB PULSE RADARS

Shouhei Kidera, Takuya Sakamoto and Toru Sato
Graduate School of Informatics, Kyoto University, Japan

ABSTRACT

Target shape estimation with UWB pulse radars is promising as an imaging technique for household robots. We have already proposed a fast imaging algorithm, SEABED based on a reversible transform BST (Boundary Scattering Transform) between the received signals and the target shape. However the target image obtained by SEABED deteriorates in a noisy environment because it utilizes a derivative of received data. In this paper, we propose a robust imaging method with an envelope of circles. In a numerical simulation, we clarify that the proposed method can realize a robust and fast imaging, which cannot be achieved by SEABED.

Keywords:UWB pulse radars, robust and fast radar imaging, an envelope of circles

1. INTRODUCTION

UWB pulse radar systems are promising as a high-resolution imaging, which is suitable and efficient for measuring techniques of household and rescue robots. Additionally, they can estimate object shapes even in a dark smoke where where optical methods cannot be applied. While many imaging algorithms for radar systems have been proposed, they require an intensive computation, which is not suitable for a realtime operation [1-4]. On the contrary, we have already proposed a fast imaging algorithm called SEABED (Shape Estimation Algorithm based on BST and Extraction of Directly scattered waves) based on a reversible transform BST between the received signals and the target shape [5], [6]. However, the image obtained by SEABED deteriorates in a noisy environment because it utilizes derivatives of the received data. For this problem, image stabilization methods have been proposed. One of them utilizes an adaptive smoothing with Gaussian filter[7], the other is based on Fractional Boundary Scattering Transform[8]. These methods are robust in a noisy environment. However, both of them utilize derivative operations, and cannot completely remove the instability.

To solve this problem, we propose a robust imaging algorithm with an envelope of circles in this paper, which does not sacrifice the fastness of SEABED. We should notice that the conventional method quoted at [9] is similar to our approach from the viewpoint that it extracts the target boundary with time delays. Additionally, this method achieves a robust imaging in a noisy environment because it does not utilize a derivative operation. However, this method can be applied only to the convex targets. In this paper, we propose a fast and robust imaging algorithm for an arbitrary shape target. We calculate circles with estimated delays for each antenna location. We utilize the principle that these circles circumscribe or inscribe the target boundary. With this principle, we prove that the target boundary is expressed as a boundary of an union and an intersection set of these circles. This method does not utilize a derivative of a received data, and enables us to realize a robust imaging for an arbitrary shaped target.

2. SYSTEM MODEL

We deal with 2-dimensional problems and TE mode waves. We assume that the target has an uniform permittivity, and surrounded by a clear boundary which is composed of smooth curves concatenated at discrete edges. We also assume that the propagation speed of the radiowave is constant and known. We assume a mono-static radar system. The induced current at the transmitting antenna is a mono-cycle pulse.

We define r-space as the real space, where targets and the antenna are located. We express r-space with the parameters (x, y). An omni-directional antenna is scanned along x axis. Both x and y are normalized by λ, which is the center wavelength of the transmitted pulse. We assume $y > 0$ for simplicity. We define $s'(X, Y)$ as the received electric field at the antenna location $(x, y) = (X, 0)$, where we define Y with the arrival time of the echo t and speed of the radio wave c as $Y = ct/(2\lambda)$. We apply the matched filter with the transmitted waveform to $s'(X, Y)$. We define $s(X, Y)$ as the output of the filter. We define d-space as the space expressed by (X, Y), and call it as a quasi wavefront.

3. CONVENTIONAL METHOD

3 .1 SEABED algorithm

We have already developed a non-parametric shape estimation algorithm called SEABED. This method utilizes a reversible transform BST between the point of r-space (x, y) and the point of d-space (X, Y), which is extracted by the output of the

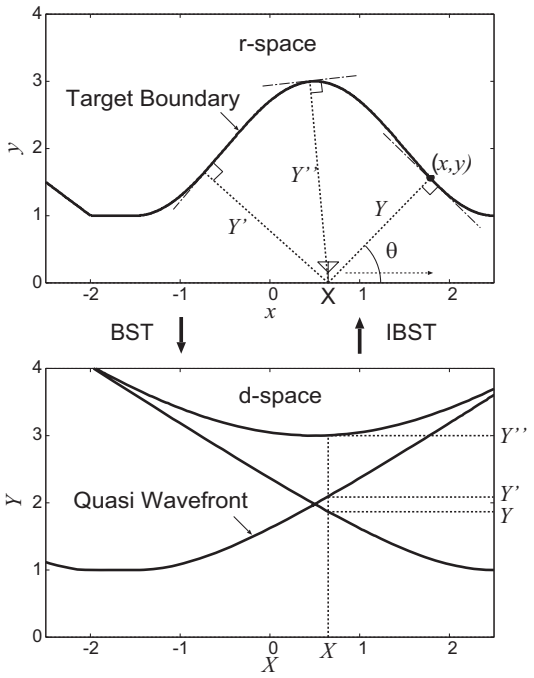

Fig. 1. *Relationship between r-space (Upper side) and d-space (Lower side).*

matched filter $s(X, Y)$. BST is expressed as

$$\left.\begin{array}{rcl} X & = & x + y\mathrm{d}y/\mathrm{d}x. \\ Y & = & y\sqrt{1 + (\mathrm{d}y/\mathrm{d}x)^2}. \end{array}\right\} \quad (1)$$

IBST (Inverse BST) is expressed as

$$\left.\begin{array}{rcl} x & = & X - Y\mathrm{d}Y/\mathrm{d}X. \\ y & = & Y\sqrt{1 - (\mathrm{d}Y/\mathrm{d}X)^2}, \end{array}\right\} \quad (2)$$

where $|\mathrm{d}Y/\mathrm{d}X| \leq 1$ holds. This transform is reversible, and gives us a complete solution for the inverse problem. Fig. 1 shows the relationship between the r-space and the d-space. IBST utilizes the characteristic that an incident wave reflects intensively in the normal direction. By utilizing IBST, SEABED enables us to estimate the target boundary directly from a quasi wavefront. SEABED has an advantage that it can directly estimate target boundaries with IBST, and achieves a fast and high resolution imaging.

3. 2. Noise tolerance of SEABED

The estimated image with SEABED easily deteriorates in a noisy environment because IBST utilizes the derivative of a quasi wavefront. In this section, we show that SEABED is unstable for a noisy environment. The signals are received at 101 locations in $-2.5\lambda \leq x \leq 2.5\lambda$. We discuss the estimation accuracy for the quasi wavefront with random error whose standard deviation is 0.005λ. This

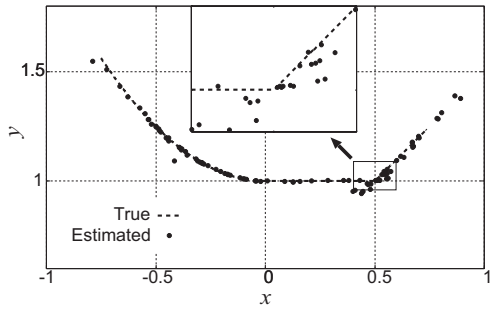

Fig. 2. *Quasi wavefront with noise (Upper side), and an estimated image with SEABED (Lower side) (Corelation length* $=0.05\lambda$*).*

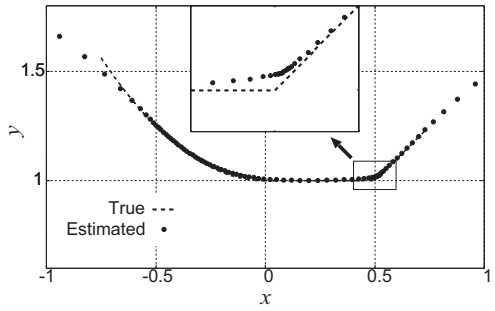

Fig. 3. *Same as Fig. 2 but corelation length is set to* 0.2λ.

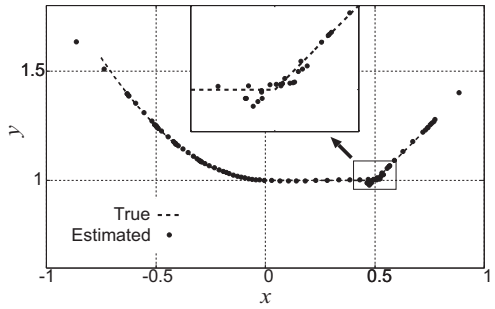

Fig. 4. *Same as Fig. 2 but corelation length is set to* 0.1λ.

simulation estimates the accuracy without the influence of other factors including waveform distortion. We smooth the quasi wavefront with Gaussian filter. Figs. 2, 4 and 3 show the estimated boundary by applying IBST to the quasi wavefront where we set a correlation length of the filter as 0.05λ, 0.2λ and 0.1λ, respectively. In Fig. 2, the estimated points have large errors around the edge. This is because the correlation length is too short. To discuss the deterioration of the image analytically, we rewrite IBST as

$$\left.\begin{array}{rcl} x & = & X + Y\cos\theta \\ y & = & Y\sin\theta \end{array}\right\}, \quad (3)$$

$$\theta = \cos^{-1}(-\mathrm{d}Y/\mathrm{d}X), \quad (0 \leq \theta < \pi),$$

where θ is expressed as in Fig. 1. Eq. (3) means that the estimated points with IBST are on the circle whose center is $(X, 0)$ and radius is Y. In the

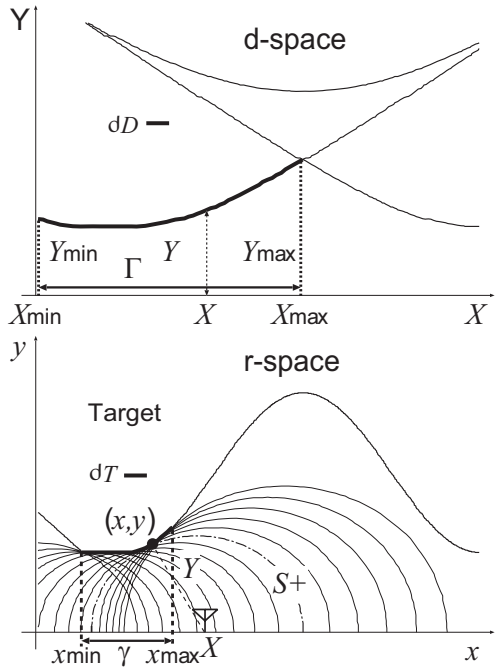

Fig. 5. *Quasi wavefront (Upper side) and a convex target boundary and an envelope of circles (Lower side).*

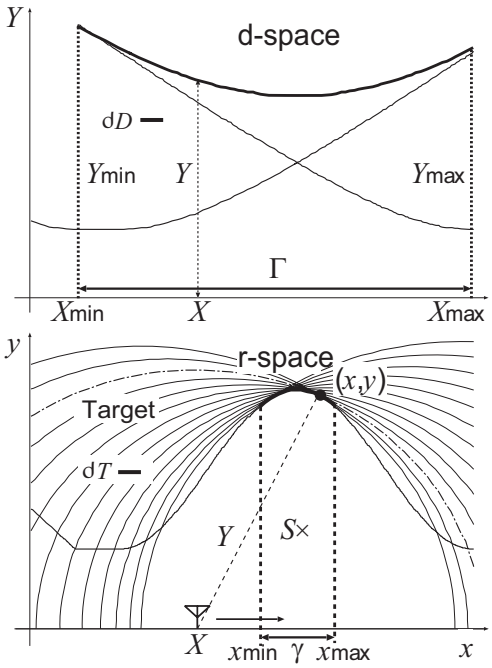

Fig. 6. *Quasi wavefront (Upper side) and a concave target boundary and an envelope of circles (Lower side).*

equation, θ is determined with $\mathrm{d}Y/\mathrm{d}X$. Therefore, the estimated point mistakingly plots along this circle in a noisy environment because the accuracy of θ strongly depends on that of $\mathrm{d}Y/\mathrm{d}X$.

While the estimated image in Fig. 3 is stable, the resolution of the image degrades especially around the edge. Accordingly, SEABED suffers from a trade-off between a stability and resolution of the estimated image. Therefore, we empirically choose the correlation length as 0.1λ which holds a resolution and a stability of the image as shown in Fig.4. However the estimated points in Fig. 4 still have errors.

To solve this trade-off of SEABED, the methods for stabilizing images have been proposed. One method is based on smoothing of the quasi wavefront, where we change the correlation length of the Gaussian filter depending on the target shape[7]. The other is based on smoothing of the data obtained in the intermediate space between the r-space and the d-space with Fractional Boundary Scattering Transform[8]. These methods achieve a robust imaging in a noisy environment. However, they cannot completely solve the above trade-off because they depend on the derivative operations.

4. PROPOSED METHOD

4. 1. A target boundary and envelopes of circles

To solve the trade-off between stability and resolution of SEABED stated in the previous section, we propose a new imaging algorithm. First, we clarify the relationship between the group of points on a target boundary and that on the envelope of the circles. We assume that the target boundary ∂T is expressed as a single-valued and differentiable function. (X, Y) is a point on ∂D, which is the quasi wavefront of ∂T. We define Γ as the domain of X for ∂D. We define $g(X,Y) = \partial x/\partial X = 1 - (\mathrm{d}Y/\mathrm{d}X)^2 - Y\mathrm{d}^2Y/\mathrm{d}X^2$, and γ as the domain of $g(X,Y)$. We define $S_{(X,Y)}$ as an open set which is an interior of the circle, which satisfies $(x-X)^2 + y^2 = Y^2$. Figs. 5 and 6 show the relationship between d-space and r-space for a convex and a concave target, respectively. If ∂D is a single-valued and continuous function, we define $S_+ = \bigcup_{X\in\Gamma} S_{(X,Y)}$ and $S_\times = \bigcap_{X\in\Gamma} S_{(X,Y)}$. We define the boundary ∂S_+ as

$$\partial S_+ = \{(x,y) \mid (x,y) \in \overline{S_+} - S_+,\ x \in \gamma,\ y > 0\}, \quad (4)$$

and $\partial S_\times$ as

$$\partial S_\times = \{(x,y) \mid (x,y) \in \overline{S_\times} - S_\times,\ x \in \gamma,\ y > 0\}, \quad (5)$$

where $\overline{S_+}$ and $\overline{S_\times}$ is a closure of S_+ and $S_\times$, respectively.

Here the next equation holds

$$\partial T = \begin{cases} \partial S_+ & (g(X,Y) > 0), \\ \partial S_\times & (g(X,Y) < 0). \end{cases} \quad (6)$$

Eq. (6) shows that ∂S_+ and $\partial S_\times$ express the target boundary as an envelope of circles depending on the sign of $g(X,Y)$ as shown in Figs. 5 and 6. We should correctly select these methods considering the sign of $g(X,Y)$. We utilize the next proposition.

Proposition 1: The necessary and sufficient condition of $g(X,Y) < 0$ is that

$$\overline{S_+} \subset \overline{S_{\max} \cup S_{\min}} \quad (7)$$

holds. Here, we define $(X_{\max}, Y_{\max})$ and $(X_{\min}, Y_{\min})$ as the point of ∂D, where $X_{\max}$ and $X_{\min}$ is the maximum and minimum value at $X \in \Gamma$, respectively as shown in Fig. 6. We define $S_{\max}$ and $S_{\min}$ express $S_{(X_{\max},Y_{\max})}$ and $S_{(X_{\min},Y_{\min})}$, respectively.

We should search the minimum number of the circles which constitute S_+. If the minimum number of circles is 2, $\partial T = \partial S_\times$ holds. Otherwise, $\partial T = \partial S_+$ holds. When a target boundary includes an edge, the edge can be estimated as the intersection point of circles $\partial S_{(X,Y)}$, where (X,Y) is transformed into the edge point (x,y) with the IBST. Therefore, the target boundary ∂T with edges can be expressed as one of ∂S_+ and $\partial S_\times$.

In our proposed method, we estimate the target boundary with an envelope of circles by utilizing these relationships. This method enables us to transform the group of points (X,Y) to the group of points (x,y) without derivative operation. Note that we receive the scattered wave which passes through a caustic point, if quasi wavefronts satisfies $g(X,Y) < 0$. In that case, a phase of the scattered waveform rotates by $\pi/2$ [6]. We can recognize this phase rotation from (X,Y) robustly with the sufficient condition of the proposition 1. We compensate this phase rotation in our proposed method to enhance the accuracy of the estimated image.

4. 2. Procedures of the proposed method

We explain the actual procedures of the proposed method as follows. Here we define $R(X,X^{'})$ as x coordinates of the intersection point of $\partial S_{(X,Y)}$ and $\partial S_{(X',Y')}$. We also define ΔX as the sampling interval of the antenna.

Step 1). Apply the matched filter to the received signals $s^{'}(X,Y)$ and obtain the output $s(X,Y)$.

Step 2). Extract quasi wavefronts as $(X,Y^{'})$ which satisfies $\partial s(X,Y)/\partial Y = 0$, $|s(X,Y)| \geq \alpha \cdot \max_Y |s(X,Y)|$. Extract (X,Y) as ∂D_{T} from $(X,Y^{'})$ which satisfies the local maximum of $Y^{'}$ for each X. Parameter α and the searching region of $Y^{'}$ is determined empirically.

Step 3). Extract a set of (X,Y) as ∂D_i from ∂D_{T} which is continuous and $|\mathrm{d}Y/\mathrm{d}X| \leq 1$ satisfies.

Step 4). Extract boundary points (x,y) on ∂S_+ $(X,Y) \in \partial D_i$ as

$$y = \max_{X \in \Gamma_i} \sqrt{Y^2 - (x-X)^2}. \quad (8)$$

where Γ_i is a domain of X where $(X,Y) \in \partial D_i$ satisfies. Count the minimum number of circles which constitute S_+, and define the number as N_{C}. If $N_{\mathrm{C}} > 2$, determine

$$\partial T_i = \partial S_+, \ (x_{\min} \leq x \leq x_{\max}), \quad (9)$$

where $x_{\min} = R(X_{\min}, X_{\min} + \Delta X)$ and $x_{\max} = R(X_{\max}, X_{\max} - \Delta X)$.
If $N_{\mathrm{C}} = 2$, compensate a phase rotation for $s(X,Y)$ by $\pi/2$ and renew the quasi wavefronts as (X,Y_{c}), and extract boundary points (x,y) on $\partial S_\times$ as

$$y = \min_{X \in \Gamma_i} \sqrt{Y_{\mathrm{c}}^2 - (x-X)^2}. \quad (10)$$

Determine

$$\partial T_i = \partial S_\times, \ (x_{\min} \leq x \leq x_{\max}), \quad (11)$$

where $x_{\min} = R(X_{\max}, X_{\max} - \Delta X)$ and $x_{\max} = R(X_{\min}, X_{\min} + \Delta X)$.

Step 5). Set $i = i + 1$, and iterate Step 3) and 4) until ∂D_{T} is empty.

Step 6). Estimate the target boundary as $\partial T = \sum_i \partial T_i$.

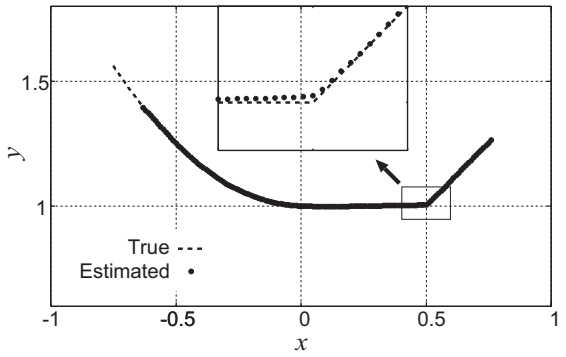

Fig. 7. *Estimated image with the proposed method for a convex target with noise.*

5. PERFORMANCE EVLUATION

We evaluate the estimation accuracy of SEABED and the proposed method. We fix the correlation length to 0.1λ from the results of 3.2. Fig. 7 shows

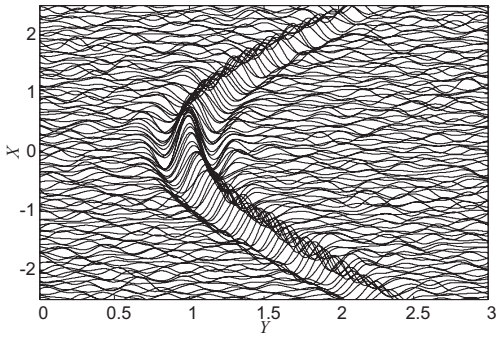

Fig. 8. *Output of the matched filter for a convex target.*

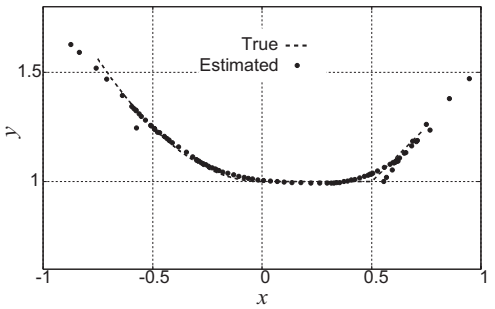

Fig. 9. *Estimated image with SEABED for a convex target with noise to* $s'(X,Y)$.

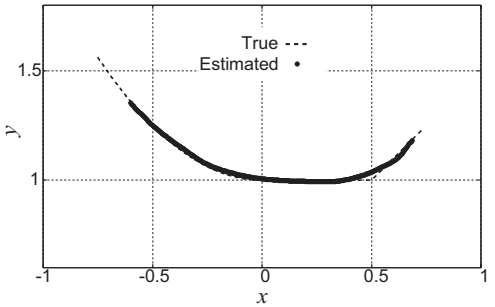

Fig. 10. *Estimated image with the proposed method for a convex target with noise to* $s'(X,Y)$.

the estimated image where we apply the proposed method to the same data as Fig. 2. The estimated image with the proposed method achieves a stable and high-resolution imaging than SEABED, especially around the edge. This is because the proposed method does not spoil the information of the inclination of the target shape.

Next, we add a white noise to the received data $s'(X,Y)$ calculated with the FDTD method. Fig. 8 shows the output of the matched filter with the transmitted waveform. In this case, S/N is about 5.5 dB. Here we define S/N as

$$\mathrm{S/N} = \frac{1}{\sigma_{\mathrm{N}}^2 (X_{\max} - X_{\min})} \int_{X_{\min}}^{X_{\max}} \max_{Y} |s(X,Y)|^2 \mathrm{d}X, \tag{12}$$

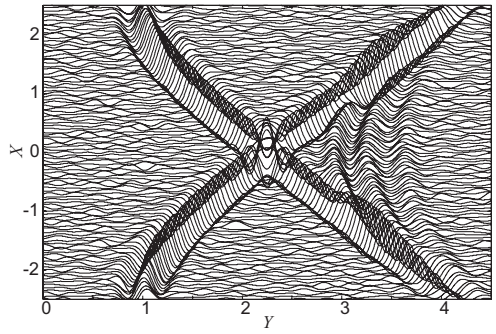

Fig. 11. *Output of the matched filter for a concave target.*

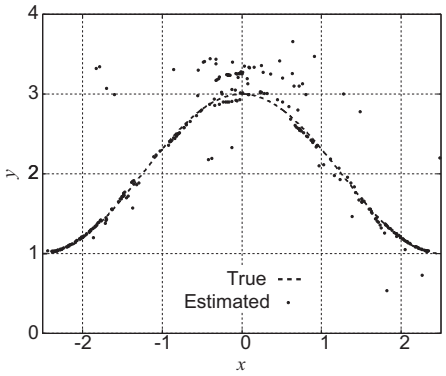

Fig. 12. *Estimated image with SEABED for a concave target with noise to* $s'(X,Y)$.

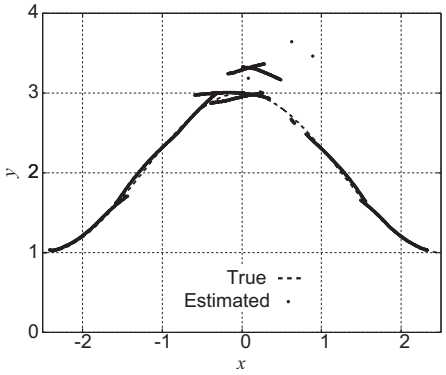

Fig. 13. *Estimated image with the proposed method for a concave target with noise to* $s'(X,Y)$.

where $X_{\max}$ and $X_{\min}$ is the maximum and minimum antenna location respectively, and σ_{N} is the standard deviation of noise. Fig. 9 and 10 show the estimated image with SEABED and the proposed method, respectively. The image of SEABED is not accurate especially around the edges of the target. On the contrary, the image obtained by the proposed method is stable, although the image around the edge is not precise compared with Fig. 7. This is because the edge diffraction waveform is different from the transmitted waveform. We should estimate the scattered waveform by using the estimated image to enhance

the accuracy [10]. This will be an important future work.

Next, we deal with the scattered signals for a concave target. Fig. 11 shows the output of the matched filter. S/N is about 8.0 dB. Figs. 12 and 13 show the estimated images for the concave target with SEABED and the proposed method, respectively. The proposed method can estimate a more stable and accurate image than SEABED. The phase rotation of the scattering at the concave surface is correctly compensated. The calculation time of the algorithm is within 0.1 sec with Xeon 3.2 GHz processor, which is short enough for real time imaging. However, false images are seen above the target boundary due to multiple scattering. This is also a future task to develop a robust algorithm without false images.

6. CONCLUSION

We proposed a stable and fast imaging method using the envelope of circles. We clarified that the convex and concave target boundary can be expressed as a boundary of union and intersection set of circles obtained by quasi wavefronts, respectively. We clarified that the proposed method can estimate stable and accurate images compared with SEABED in numerical simulations. Besides, the proposed method achieves a fast imaging like SEABED. It is an important future work to extend this algorithm to 3-dimensional problem, and achieve a higher resolution to compensate the waveform distortion.

ACKNOWLEDGEMENT

This work is supported in part by the 21st Century COE Program (Grant No. 14213201).

References

[1] C. Chiu, C. Li, and W. Chan, "Image reconstruction of a buried conductor by the genetic algorithm," *IEICE Trans. Electron.*, vol. E84-C, no. 12, pp. 1946–1951, 2001.

[2] T. Takenaka, H. Jia, and T. Tanaka, "Microwave imaging of an anisotropic cylindrical object by a forward-backward time-stepping method," *IEICE Trans. Electron.*, vol. E84-C, no. pp. 1910–1916, 2001.

[3] T. Sato, K. Takeda, T. Nagamatsu, T. Wakayama, I. Kimura and T. Shinbo, "Automatic signal processing of front monitor radar for tunneling machines," *IEEE Trans. Geosci. Remote Sens.*, vol.35, no.2, pp.354-359, 1997.

[4] T. Sato, T. Wakayama, and K. Takemura, "An imaging algorithm of objects embedded in a lossy dispersive medium for subsurface radar data processing," *IEEE Trans. Geosci. Remote Sens.*, vol.38, no.1, pp.296–303, 2000.

[5] T. Sakamoto and T. Sato, "A target shape estimation algorithm for pulse radar systems based on boundary scattering transform," *IEICE Trans. Commun.*, vol.E87-B, no.5, pp. 1357–1365, 2004.

[6] T. Sakamoto and T. Sato, "A phase compensation algorithm for high-resolution pulse radar systems," *IEICE Trans. Commun.*, vol.E87-B, no.6, pp. 1631–1638, 2004.

[7] T. Sakamoto and T. Sato, "An experimental study on a fast and accurate 3-D imaging algorithm for UWB pulse radar systems," 28th General Assembly of International Union of Radio Science (URSI), F05.7, Oct, 2005.

[8] T. Sakamoto and T. Sato, "An accurate shape estimation method with the adaptive Fractional Boundary Scattering Transform for UWB pulse radars," (in Japanese) 34 th. Electromagnetic Theory Symposium, EMT–05-57, Nov, 2005.

[9] M. Tsunasaki, H. Mitsumoto, and M. Kominami, "Aperture estimation of the underground pipes by ellipse estimation from ground penetrating radar image," (in Japanese) Technical Report of IEICE, SANE2003–52, Sep, 2003.

[10] S. Kidera, T. Sakamoto, and T. Sato, "A high-resolution imaging algorithm based on scattered waveform estimation for UWB pulse radar systems," Proc. 2005 IEEE International Geoscience and Remote Sensing Symposium, pp. 1725–1728, Jul, 2005.